Monthly Notices of the ROYAL ASTRONOMICAL SOCIETY

MNRAS **517,** 5406–5412 (2022) https://doi.org/10.1093/mnras/stac2883
Advance Access publication 2022 October 10

TRAPUM upper limits on pulsed radio emission for SMC X-ray pulsar J0058−7218

E. Carli [1]★ L. Levin [1] B. W. Stappers [1] E. D. Barr [2] R. P. Breton [1] S. Buchner [3] M. Burgay [4] M. Kramer [2] P. V. Padmanabh [2,5] A. Possenti [4] V. Venkatraman Krishnan [2] J. Behrend [2] D. J. Champion [2] W. Chen [2] and Y. P. Men [2]

[1]*Jodrell Bank Centre for Astrophysics, Department of Physics and Astronomy, The University of Manchester, Manchester M13 9PL, UK*
[2]*Max-Planck-Institut für Radioastronomie, Auf dem Hügel 69, D-53121 Bonn, Germany*
[3]*South African Radio Astronomy Observatory (SARAO), 2 Fir Street, Black River Park, Observatory, Cape Town 7925, South Africa*
[4]*INAF-Osservatorio Astronomico di Cagliari, via della Scienza 5, I-09047 Selargius, Italy*
[5]*Max-Planck-Institut für Gravitationsphysik (Albert-Einstein-Institut), D-30167 Hannover, Germany*

Accepted 2022 October 4. Received 2022 October 4; in original form 2022 July 29

ABSTRACT

The TRAPUM collaboration has used the MeerKAT telescope to conduct a search for pulsed radio emission from the young Small Magellanic Cloud pulsar J0058−7218 located in the supernova remnant IKT 16, following its discovery in X-rays with *XMM–Newton*. We report no significant detection of dispersed, pulsed radio emission from this source in three 2-h *L*-band observations using the core dishes of MeerKAT, setting an upper limit of 7.0 μJy on its mean flux density at 1284 MHz. This is nearly seven times deeper than previous radio searches for this pulsar in Parkes *L*-band observations. This suggests that the radio emission of PSR J0058−7218 is not beamed towards Earth or that PSR J0058−7218 is similar to a handful of Pulsar Wind Nebulae systems that have a very low radio efficiency, such as PSR B0540−6919, the Large Magellanic Cloud Crab pulsar analogue. We have also searched for bright, dispersed, single radio pulses and found no candidates above a fluence of 93 mJy ms at 1284 MHz.

Key words: pulsars: individual: PSR J0058−7218.

1 INTRODUCTION

The Magellanic Clouds are the only galaxies outside our own in which radio pulsars have been discovered to date. They are nearby galaxies that are unobstructed by the Galactic plane, therefore they are a good target for extragalactic pulsar searches. Indeed, the Small Magellanic Cloud (SMC) is just 60 kpc away (Karachentsev et al. 2004), and the expected Milky Way dispersion measure (DM) contribution in its direction is low: about 30 pc cm^{-3} according to the YMW2016 electron density model (Yao, Manchester & Wang 2017), and 42 pc cm^{-3} according to the NE2001 model (Cordes & Lazio 2002). There was a recent episode of stellar formation in the SMC about 40 Myr ago (Harris & Zaritsky 2004), which led to an abundance of young systems per unit mass compared to the Milky Way. In particular, the SMC hosts many supernova remnants (18 confirmed SNRs in Maggi et al. 2019), which can contain young neutron stars. Due to their rarity in the Milky Way's older population,[1] the discovery of young pulsars is scientifically interesting. Among them, magnetars (which have the highest known stellar magnetic fields) are prized for a variety of fundamental physics and astrophysics investigations (Esposito, Rea & Israel 2021), including as one of the progenitors of fast radio bursts (Bochenek et al. 2020; Caleb & Keane 2021). Each Magellanic Cloud hosts one known magnetar (Helfand & Long 1979; Lamb et al. 2002). Additionally, extragalactic pulsars are sought after for insights on the impact of different galactic properties on neutron star formation, such as the impact of metallicity and star formation history on stellar mass and supernova physics (Heger et al. 2003; Titus et al. 2020).

There are seven published radio pulsars in the SMC and all have been discovered with the Parkes 64-m single dish radio telescope in Australia, by McConnell et al. (1991, one pulsar), Crawford et al. (2001, one), Manchester et al. (2006, three), and Titus et al. (2019, two). Their median DM is around 115 pc cm^{-3}. The radio emission from these pulsars is powered by their rapid rotation. This can also power hard X-ray emission when the pulsar is young and most rapidly rotating. The X-ray emission has a characteristic hard power-law spectrum (Becker & Trümper 1997, and references therein). Only two young[2] pulsars have been discovered in the SMC, both in the X-ray band only: CXOU J010043.1−721134 (a magnetar; Lamb et al.

★ E-mail: emma.carli@postgrad.manchester.ac.uk

[1]In the Australia Telescope National Facility (ATNF) pulsar catalogue (Manchester et al. 2005), only about ≃180 pulsars out of ≃2500 with a catalogued characteristic age are younger than 120 kyr.

[2]All other published non-magnetar pulsars in the SMC are over 1 Myr in characteristic age (Manchester et al. 2005).

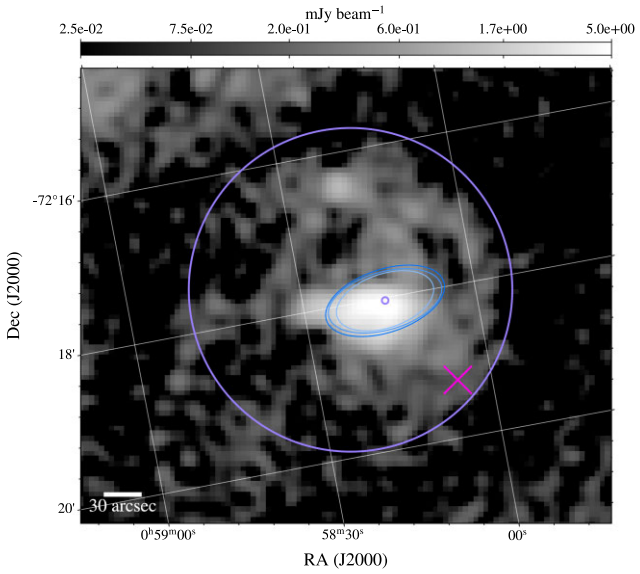

Figure 1. Regions of interest are overlaid on a 1320 MHz ASKAP image of the SMC (Joseph et al. 2019). The morphology of the composite SNR is delineated by purple circles. The largest purple circle delimits the SNR shell as catalogued by Maggi et al. (2019). It contains a comparatively bright feature around the 5.2 arcsec diameter PWN (smallest purple circle, Maitra et al. 2015). Our observed MeerKAT beams are shown at 50 per cent sensitivity as blue ellipses, simulated with MOSAIC (Chen et al. 2021). The innermost beam is OBS1 and the outermost beam is OBS3 (cf. Table 1). They are centred on the PWN position. The centre of the Parkes telescope beam from the Titus et al. (2019) survey is shown as a pink cross. The 14 arcmin Parkes half-power beamwidth lies outside the figure. This figure was generated with the APLPY PYTHON package.

2002), and most recently, PSR J0058−7218 (Maitra et al. 2021). In this paper, we describe the follow-up radio observations of the latter with MeerKAT.

PSR J0058−7218 is situated in the supernova remnant (SNR) IKT 16 (Inoue, Koyama & Tanaka 1983), also known as DEM S 103 (Davies, Elliott & Meaburn 1976). The remnant was first identified as an Hα emission nebula LHA 115-N 66 in Henize (1956). The first radio observations of the nebula were made by Mills & Aller (1971), and it was tentatively suggested to be a non-thermal radio source by Clarke, Little & Mills (1976). It was catalogued as 1E0057.6−7228 with the first X-ray detection of the system by Seward & Mitchell (1981). Mills et al. (1982) conducted further radio observations which led to the proposition that DEM S 103 was a tentative SNR candidate. It was officially declared a candidate SNR based on soft X-ray observations by Inoue et al. (1983), and subsequently named IKT 16. A radio and Hα study by Mathewson et al. (1984) confirmed that IKT 16 is an SNR, which they found is in the Sedov evolutionary phase. Further insights as to the nature of the system were made possible by the launch of the *XMM–Newton* and *Chandra* X-ray observatories. Van Der Heyden, Bleeker & Kaastra (2004) identified a hard X-ray source within the SNR in a single *XMM* exposure, but it was too faint to be further characterized. After eight additional *XMM–Newton* observations, Owen et al. (2011) identified the hard X-ray source as a tentative pulsar wind nebula (PWN), within a larger, extended radio source from ATCA and MOST radio images (inside the SNR, see Fig. 1). As the PWN is offset from the centre of the SNR, they suggested the existence of a pulsar in motion, with a transverse kick velocity of 580 km s^{-1}. Using adiabatic Sedov modelling, they estimated the age of the SNR to be 14.7 kyr. The putative pulsar emission could not be resolved from the PWN at the time.

Maitra et al. (2015) confirmed the existence of the PWN with *Chandra* observations, resolving a putative pulsar at its centre in hard X-rays. IKT 16 was thus defined as a 'composite SNR', where there is non-thermal emission from both the SNR shell in radio and the hard X-ray point source within the PWN. The latter's measured X-ray spectral index implied a young, rotation-powered pulsar with non-thermal radiation from the pulsar magnetosphere (e.g. Becker & Trümper 1997; Wang & Zhao 2004). Using a similar method as Kargaltsev et al. (2008) using the X-ray luminosities of the PWN and point source, Maitra et al. (2015) estimated the period of the putative pulsar to be of the order of 100 ms with a period derivative $\simeq 10^{-13}$. Maitra et al. (2015) characterized the morphology of the system: the PWN is a 5.2 arcsec elongated X-ray feature at RA(J2000) = $00^h58^m16\overset{s}{.}824 \pm 0\overset{s}{.}1$ Dec(J2000) = $-72°18'05\overset{''}{.}32 \pm 0\overset{''}{.}2$ (*Chandra* position). The putative pulsar (hard X-ray point source) is consistent with the PWN centre, at RA(J2000) = $00^h58^m16\overset{s}{.}85$ Dec(J2000) = $-72°18'05\overset{''}{.}60 \pm 0\overset{''}{.}6$ (*Chandra* position). The PWN is located within a larger radio feature, which Maitra et al. (2015) described as two lobes about the PWN each 20 ± 5 arcsec in extent (see Fig. 1), from a high-resolution ATCA 2.1 GHz image. They concluded that the PWN is in expansion in the cold SNR ejecta. No radio point source was detected near the X-ray point source.

The first dedicated search for a radio pulsar in IKT 16 was conducted by Titus et al. (2019) with the Parkes radio telescope, in two 4-h observations with a beam of the Parkes Multi-Beam receiver (Staveley-Smith et al. 1996) placed 1.4 arcmin from the position of the putative pulsar (see Fig. 1). The observations had a 400 MHz bandwidth centred on 1382 MHz (Berkeley–Parkes–Swinburne data recorder: Keith et al. 2010; McMahon 2011). They carried out a Fourier domain search with PRESTO (Ransom, Eikenberry & Middleditch 2002; Ransom 2011) for DMs up to 660 pc cm^{-3} and a fast-folding search with RIPTIDE for DMs up to 400 pc cm^{-3} (Morello et al. 2020). PSR J0058−7218 was not detected down to S/N = 8, corresponding to a 1400 MHz flux density limit of 36 μJy. This limit takes into account the sensitivity loss from the putative pulsar being off-centre in the beam and assumes a 5 per cent duty cycle. With a 7 K sky temperature contribution included (Zheng et al. 2017), the flux density limit is 47 μJy.

The 21.7 ms pulsar J0058−7218 was finally discovered in X-rays by Maitra et al. (2021) in 2020 *XMM–Newton* EPIC camera observations. They measured a hard X-ray spectral index of 1.4 ± 0.1 and a single peak pulse shape. They determined an ephemeris using the pulsar position from Maitra et al. (2015). The pulsar has a high period derivative of $\simeq 3 \times 10^{-14}$, giving a young characteristic age of about 12 kyr (in line with the SNR Sedov age from Owen et al. 2011), and a high spin-down luminosity $\dot{E} = 1.1 \times 10^{38}$ erg s^{-1}. The inferred surface magnetic field of $B_{\rm surf} = 8 \times 10^{11}$ G excludes that PSR J0058−7218 is a magnetar (Esposito et al. 2021). Maitra et al. (2021) conducted multiwavelength searches of PSR J0058−7218: they reported no gamma-ray pulsations in the most recent *Fermi* LAT data set, and no radio pulsations in a reprocessing of the Titus et al. (2019) Parkes data. They folded the data at the predicted topocentric period of the pulsar using DSPSR and searched the folded data for the highest S/N profile over DMs 0–1000 pc cm^{-3} with PSRCHIVE's `pdmp` tool (Hotan, Van Straten & Manchester 2004; Van Straten & Bailes 2011). They quote a better flux density limit than Titus et al. (2019), 15 μJy at 1400 MHz, as they use a lower signal-to-noise ratio (S/N) limit of 5 in their folding search, and do not take into account the sensitivity loss from the pulsar being off-centre in the Parkes beam (M. Pilia, private communication). Adding this

Table 1. Characteristics of the MeerKAT coherent beam observations of PSR J0058−7218. For each observation, one coherent beam is placed at the centre of the PWN as defined by Maitra et al. (2015), RA(J2000) = $00^h58^m16\overset{s}{.}824$ Dec(J2000) = $-72^\circ18'05\overset{''}{.}32$. The coherent beam is placed within the MeerKAT primary incoherent beam, which pointing location is given in Right Ascension and Declination (J2000). The coherent beam major axes are given in arcseconds in the Right Ascension and Declination directions, with the ellipse position angle.

Observation number and date	Primary incoherent beam location	Number of dishes	Coherent beam size (50 per cent sensitivity)	Sampling time	Processing
OBS1	$0^h55^m14\overset{s}{.}6910$	40	$40\overset{''}{.}0$, $21\overset{''}{.}3$	76 μs	Pulsar search
14 Jan 2021	$-72^\circ26'06\overset{''}{.}899$		$9\overset{\circ}{.}2$		Fold on downsampled data
OBS2	$0^h55^m14\overset{s}{.}6910$	44	$46\overset{''}{.}2$, $22\overset{''}{.}9$	153 μs	Pulsar search fold
24 Apr 2021	$-72^\circ26'06\overset{''}{.}899$		$6\overset{\circ}{.}6$		Single pulse search
OBS3	$0^h57^m21\overset{s}{.}2370$	44	$48\overset{''}{.}9$, $24\overset{''}{.}9$	153 μs	Pulsar search fold
27 Oct 2021	$-71^\circ52'35\overset{''}{.}195$		$9\overset{\circ}{.}0$		Single pulse search

sensitivity loss, a sky temperature contribution of 7 K, and an S/N cut of 7 to compare with our own searches, this limit becomes 41 μJy at 1400 MHz. They also did not find any single pulses in this data set with HEIMDALL over DMs 0–1000 pc cm^{-3} (Barsdell et al. 2012). Using the survey parameters from Titus et al. (2019), and taking into account the sensitivity loss from the pulsar being off-centre in the Parkes beam, a sky temperature contribution of 7 K, and a S/N cut of 8 to compare with our own searches, we find their single pulse search has a limiting fluence of 821 mJy ms[3] for a 1 ms pulse width at 1400 MHz (with a 1 ms integration time).

TRAPUM (TRAnsients and PUlsars with MeerKAT) is a Large Survey Project of the MeerKAT telescope (trapum.org; Stappers & Kramer 2016). One of TRAPUM's science goals is to find new extragalactic pulsars. Thus, the collaboration is currently conducting a survey of the SMC with the MeerKAT telescope. PSR J0058−7218 and its PWN are located within several of the survey's pointings. The X-ray pulsar discovery in Maitra et al. (2021) was published during our survey, after one observation of the PWN was made.

2 OBSERVATIONS AND DATA REDUCTION

We placed one coherent beam at the centre of the PWN[4] (as defined by Maitra et al. 2015: RA(J2000) = $00^h58^m16\overset{s}{.}824$ Dec(J2000) = $-72^\circ18'05\overset{''}{.}32$), in three multibeam observations as part of our SMC survey. The beams were formed using the core dishes of MeerKAT (40 or 44 dishes out of 64) with a maximum baseline length of 1 km. This reduction from the full array's 8 km maximum baseline strikes a good balance between beam area and sensitivity (Chen et al. 2021). We carried out the three 2-h observations at *L* band (856–1712 MHz, 856 MHz bandwidth), with 2048 frequency channels, and a beam area large enough to cover the *Chandra* hard X-ray pulsar position error: RA(J2000) = $00^h58^m16\overset{s}{.}85$ Dec(J2000) = $-72^\circ18'05\overset{''}{.}60 \pm 0\overset{''}{.}6$ (Maitra et al. 2015). The characteristics of the individual observations are given in Table 1 and Fig. 1.

We have run a pulsar search on all three observations of the PWN, as part of the standard processing used in the TRAPUM SMC survey. Radio frequency interference (RFI) cleaning was performed with a combination of IQRM (Morello, Rajwade & Stappers 2021), PRESTO's `rfifind`, and PULSARX's `filtool`.[5] As this was part of a multibeam search we also used a multibeam RFI filter MULTITRAPUM.[6] The latter is a wrapper of `rfifind` which removes signals detected in several beams with sufficient spatial separation. The de-dispersion plan was computed with PRESTO's `DDplan.py` script. We used the DEDISP library (Barsdell et al. 2012; Levin 2012) for dedispersion over DMs from 50 to 350 pc cm^{-3} as part of the PEASOUP[7] suite, a GPU-based time-domain linear acceleration pulsar searching software. The DM range was chosen based on the median DM of the published pulsars in the SMC, around 115 pc cm^{-3}. The PWN and SNR material could add a contribution to the DM. Using PEASOUP, the 2-h long data were searched with no acceleration, while 20-min segments were searched with accelerations up to |50| m s^{-2}, to allow for binary systems[8] (assuming constant acceleration). We chose an acceleration tolerance parameter of 10 per cent (Levin 2012). This means the acceleration broadening from one acceleration step to the next cannot exceed 10 per cent of the combined pulse smearing due to sampling time, intra-channel frequency dispersion, and de-dispersion step size. The 2-h timeseries were zero-padded to the next nearest power of 2, 2^{26}, resulting in a better resolved Fourier spectrum. Candidates were harmonically summed by PEASOUP up to the eighth harmonic (Taylor & Huguenin 1969). The resulting candidates were then sifted, i.e. clustered in DM, period, acceleration, and harmonics. A first round of sifting was performed directly by PEASOUP, which returned on average around 10 000 candidates in the beam for one observation. It was followed by multibeam spatial sifting,[9] which uses the expected spatial relationship of real sources to identify RFI, after which about 3000 candidates remained. We decided to only keep candidates with periods longer than eight time samples (1.216 ms) for OBS2 and OBS3, which had a sampling time of 153 μs (cf. Table 1). For OBS1, that had a 76 μs sampling time, the shortest period folded was the PEASOUP default minimum period searched of 0.91 ms. The longest period searched by PEASOUP is 10 s. We folded about 1000 PEASOUP candidates in these period ranges with a spectral S/N above 9 using PULSARX's `psrfold_fil`. `psrfold_fil` cleans the full resolution data before folding and applies CLFD on the folded data.[10] The folds were searched for the highest S/N profile over a so-called 'natural' range around the candidate period, period derivative, DM, and acceleration. We then partially classified the folded candidates with PICS (a pulsar image-based classification system based on machine learning; Zhu et al.

[3]In Maitra et al. (2021), a fluence limit of 160 mJy ms down to S/N = 5 is quoted. The beam correction and sky temperature are again not taken into account. Additionally, the correction factor accounting for data acquisition system imperfections is not used (M. Pilia, private communication).
[4]Maitra et al. (2015) showed that the pulsar position is consistent with the centre of the PWN (see Section 1).
[5]https://github.com/ypmen/PulsarX by Yunpeng Men
[6]https://github.com/mcbernadich/multiTRAPUM by Miquel Colom i Bernadich
[7]https://github.com/ewanbarr/peasoup by Ewan Barr
[8]We already know from Maitra et al. (2021) and Ho et al. (2022) that the system is not significantly accelerated, but acceleration searching is part of standard TRAPUM SMC Survey processing, and OBS1 was processed before the discovery of PSR J0058−7218 was published in Maitra et al. (2021).
[9]https://github.com/prajwalvp/candidate_filter by Lars Künkel
[10]https://github.com/v-morello/clfd by Vincent Morello

2014). We used a minimum score of 10 per cent pulsar-like for both the original and TRAPUM training sets (Voraganti Padmanabh 2021), as well as a minimum folded S/N of 7. This returned a handful of candidates in the beam for each observation, all of which were consistent with RFI or noise. The original PEASOUP candidates files, where the spectral S/N was limited to above 8, were inspected in case the pulsar candidate had a lower spectral S/N than our folding cut-off of 9, or was lost in sifting, but no periodic signals were found at PSR J0058−7218's period. More information about the TRAPUM search pipeline can be found in chapter 3 of Voraganti Padmanabh (2021).

The discovery of PSR J0058−7218 was published in Maitra et al. (2021) after the full resolution data for OBS1 were deleted.[11] We used the ephemeris provided[12] to fold a downsampled OBS1 and the full resolution OBS2 and OBS3 with DSPSR (which calls on TEMPO2, Hobbs, Edwards & Manchester 2006, to predict the pulsar period). The folded data were cleaned with PRESTO's `rfifind` frequency channel mask from the full resolution data, CLFD, and PSRCHIVE. We then searched for the highest S/N profile in the folded data with PSRCHIVE's `pdmp` tool up to a DM of 500 pc cm^{-3}, with a period range of ± 1 µs, which is three orders of magnitude greater than the period error determined by Maitra et al. (2021). This should also cover any period derivative inaccuracies. We also ran folding searches up to a DM of 1000 pc cm^{-3} with PULSARX's `psrfold_fil` on the downsampled data from OBS1 and the full resolution OBS2 and OBS3 data. We applied a `rfifind` frequency channel mask from the full resolution data. `psrfold_fil` cleans the full resolution data before folding and applies CLFD on the folded data. The folds were searched for the highest S/N profile over a so-called natural range around the ephemeris-predicted topocentric spin frequency $\left(\pm\frac{1}{T_{obs}}\right)$ and spin-down rate $\left(\pm\frac{2}{T_{obs}^2}\right)$, where T_{obs} is the observation length in seconds. This is three and four orders of magnitudes larger than the error bounds from Maitra et al. (2021), respectively. Both folding procedures were split into several searches, each centred on a DM, with a range of ± 5 pc cm^{-3} for `pdmp`, and a DM range so that the maximum dispersion delay is one pulse period over the whole observation for `psrfold_fil`. The DMs were spaced by 10 pc cm^{-3} over the entire DM range, and returned no significant pulsations at the appropriate parameters.

A new ephemeris for PSR J0058−7218 was published in Ho et al. (2022) from *NICER* X-ray observations (Gendreau et al. 2016). This ephemeris has smaller error ranges on its parameters as it covers an 8-month X-ray timing period, while the ephemeris from Maitra et al. (2021) used data from 2020 *XMM–Newton* EPIC camera observations that only spanned 1.4 d. This consolidated the proposed age and $\dot{E}$ of PSR J0058−7218. Ho et al. (2022) noted that this is the fourth highest $\dot{E}$ known. The new ephemeris also contains a second period derivative. We repeated the same folding search procedure as before with this new ephemeris, except for the `rfifind` frequency channel mask which was not applied (PULSARX's `filtool` was run directly on the data instead) and the period derivative plane was not searched (only DM and period). We also used higher resolution folded data. Again, there were no significant pulsations at the appropriate parameters.

Young pulsars like PSR J0058−7218 can emit giant narrow pulses (e.g. the LMC Crab pulsar twin, Johnston & Romani 2003). If PSR J0058−7218 is too faint to be detected by MeerKAT in 2-h observations, single pulses that are orders of magnitude stronger than average may still be detected. We thus searched for single pulses with TRANSIENTX[13] on the full resolution data from OBS2 and OBS3, cleaned by `rfifind` and PULSARX's `filtool`. We used a 100 ms maximum search width over DMs 0–5000 pc cm^{-3}. No pulses were returned down to S/N = 8. Similarly, we ran a HEIMDALL search on the same data, cleaned by IQRM and `rfifind`. We chose a maximum boxcar width of 157 ms over DMs 25–5000 pc cm^{-3}. We discarded any pulses with widths wider than 50 per cent of PSR J0058−7218's period, as giant pulses are typically narrow (e.g. Crawford et al. 2009). We used DSPSR and PSRCHIVE to extract single pulses, search in DM for the highest S/N profile and plot the candidates. Inspection of all the candidates above S/N = 8 indicated they were consistent with RFI or noise.

3 UPPER LIMITS AND DISCUSSION

We calculate a radio *L*-band flux density upper limit for PSR J0058−7218 with the folds performed on the data from OBS2, in which the pointing location of MeerKAT's primary incoherent beam was closest to the pulsar and 44 dishes were used (see Table 1). Owing to the separation between the coherent beam placed on PSR J0058−7218 and the centre of the primary beam, the gain was decreased to ≃85 per cent of its full value (using a primary beam model based on Asad et al. 2021). Taking this into account, the radiometer equation applied to pulsar observations (Lorimer & Kramer 2005) yields a flux density upper limit of $S_{1284\,\mathrm{MHz}} = 7.0$ µJy. We assume a 5 per cent pulsar duty cycle and a minimum folded S/N of 7 to be able to distinguish the signal by eye. We use the MeerKAT system temperature (≃18 K), a sky temperature of 7 K (Zheng et al. 2017), and a gain of ≃1.925 K Jy^{-1} for the 44 core dishes (Bailes et al. 2020) at the centre of the pointing (primary beam location). We assume that a correction factor accounting for any data acquisition system imperfections is not needed. Using the flux density from the ASKAP image shown in Fig. 1, we take the faint remnant's contribution to the system temperature as negligible. Assuming a power-law radio spectral index of -1.60 ± 0.54 (Jankowski et al. 2018), the radio flux density upper limits at 1400 MHz are $S_{1400\,\mathrm{MHz}} = 6.1 \pm 0.3$ µJy.[14] Our 1400 MHz flux density limit is ≃6.7 times deeper than the 41 µJy limit from Maitra et al. (2021).

Similarly, the limiting fluence for the single pulse search on OBS2 down to S/N = 8 is $S_{\mathrm{pulse},1284\,\mathrm{MHz}} = 93$ mJy ms, for a 1 ms pulse width (and a 1 ms integration time). This takes into account the primary beam sensitivity loss and the sky temperature contribution. Again, this greatly improves the previous upper limit from Maitra et al. (2021) of 821 mJy ms, resulting from a transient search on Titus et al. (2019) Parkes data with a central frequency of 1382 MHz.

If PSR J0058−7218's radio beam is sweeping across our line of sight, the pulsar could be too faint to be detected in 2 h with the core dishes of MeerKAT. The upper limit on the flux density of the pulsar at 1400 MHz translates to a radio pseudo-luminosity

[11] As the raw data are too voluminous to keep, we stored a RFI-cleaned downsampled (512 channels each de-dispersed at a DM of 115 pc cm^{-3} and 1.225 ms sampling time) version of OBS1.

[12] Even if the ephemeris did not extend to our observations, the pulsar search could detect the source within our survey pipeline limits.

[13] https://github.com/ypmen/TransientX by Yunpeng Men

[14] Titus et al. (2020) calculated the TRAPUM search limiting flux density to be 12 µJy at 1400 MHz with different assumptions, notably a smaller bandwidth, higher S/N cut, and lower sensitivity (N. Titus, private communication).

upper limit of $L_{\rm pseudo,1400\,MHz} = S_{1400\,\rm MHz} \times D^2 = 22\,\rm mJy\,kpc^2$, assuming an approximate distance to the pulsar of $D = 60\,\rm kpc$ (Karachentsev et al. 2004), and a power-law radio spectral index of −1.6. According to the ATNF pulsar data base, for pulsars with a catalogued pseudo-luminosity, approximately 75 per cent of all pulsars and more than 50 per cent of young pulsars with a characteristic age lower than 120 kyr have a lower pseudo-luminosity than this upper limit for PSR J0058−7218 (Manchester et al. 2005). Since we did not detect any giant single pulses either, PSR J0058−7218 was either not emitting giant pulses during our observations or its radio beam is not sweeping our line of sight.

Maitra et al. (2021) measured a pulsed, non-thermal[15] X-ray luminosity for PSR J0058−7218 of $1.6(1) \times 10^{35}\,\rm erg\,s^{-1}$ in the energy band 0.2–12 keV, assuming a distance of 60 kpc (Karachentsev et al. 2004). Furthermore, they determined the pulsar spin-down luminosity $\dot{E} = 1.1 \times 10^{38}\,\rm erg\,s^{-1}$. Thus, they state that the X-ray radiation efficiency of the pulsar, $\eta_{\rm x} = \frac{L_{\rm x}}{\dot{E}}$ is of the order of 10^{-3}. This fits well with the expected relationship between $L_{\rm x}$ and $\dot{E}$ (Shibata et al. 2016). The ratio of PSR J0058−7218's X-ray luminosity to its radio luminosity upper limit, $\frac{L_{\rm x}}{L_{\rm radio}}$, is of the order of 10^5. Maitra et al. (2021) and Ho et al. (2022) did not detect any statistically significant pulsed gamma-ray flux from PSR J0058−7218. They could not provide a pulsed gamma-ray luminosity upper limit, so it is not possible to constrain the gamma-ray efficiency.

Using a general formula for pulsar luminosity derived in Lorimer & Kramer (2005) and used in Szary et al. (2014) to broadly compare the radio emission efficiencies of pulsars, we find that the radio luminosity upper limit for PSR J0058−7218 is $L_{\rm radio} = 7.4 \times 10^{27} \times L_{\rm pseudo,1400\,MHz} = 1.6 \pm 0.1 \times 10^{29}\,\rm erg\,s^{-1}$. Thus the radio radiation efficiency of the pulsar is lower than $\eta_{\rm radio} = \frac{L_{\rm radio}}{\dot{E}} = 1.5 \pm 0.1 \times 10^{-9}$. The ranges are due to the assumed radio spectral index, -1.60 ± 0.54 (Jankowski et al. 2018). According to the ATNF pulsar data base, only eight pulsars out of ≃2000 with catalogued radio and spin-down luminosities have a lower radio radiation efficiency than this upper limit, although we note that it is speculative to use this general pulsar luminosity formula to compare individual pulsars, especially with uncertain distance estimates. They are all young[16] Milky Way pulsars with pulsed high-energy emission (gamma-ray and/or X-ray), high $\dot{E}$ ($>10^{36}$ erg s^{-1}) and most have associated PWNe and/or SNRs. Notably, the Crab pulsar is among these systems. It is the only pulsar out of the eight with known giant pulses. Those detected in X-ray pulsations all have an X-ray efficiency $\eta_{\rm x}$ that fits well with the expected relationship between $L_{\rm x}$ and $\dot{E}$ (Shibata et al. 2016). PSR J0058−7218 could thus be a similar system with a very low radio emission efficiency. Szary et al. (2014) show that radio efficiency generally increases with pulsar age, due to the constancy of their radio luminosity and decline in spin-down luminosity, which is a important insight into the radio emission mechanism.

Indeed, when considering the $\eta_{\rm radio}$-$\dot{E}$ relationship presented in Szary et al. (2014) with the latest version of the ATNF pulsar catalogue, as presented in Fig. 2, PSR J0058−7218's upper limit on $\eta_{\rm radio}$ (and lower values down to $\eta_{\rm radio} \simeq 10^{-11}$) fits within the large relationship scatter, among young pulsars with pulsed high-energy radiation and SNR association. This plot was created with pulsars from the ATNF data base with a catalogued distance and 1400 MHz flux density to calculate $L_{\rm radio}$; and with a catalogued period derivative to calculate $\dot{E} = 4\pi^2 \times 10^{45} \times \dot{P} P^{-3}$. The resulting radio emission efficiencies $0 < \eta_{\rm radio} < 1$ were plotted, removing anomalous values. Note that only so-called normal spin-powered pulsars are shown, excluding millisecond pulsars, pulsars in globular clusters, rapidly rotating radio transients (RRATs), pulsars in binary systems, and magnetars.

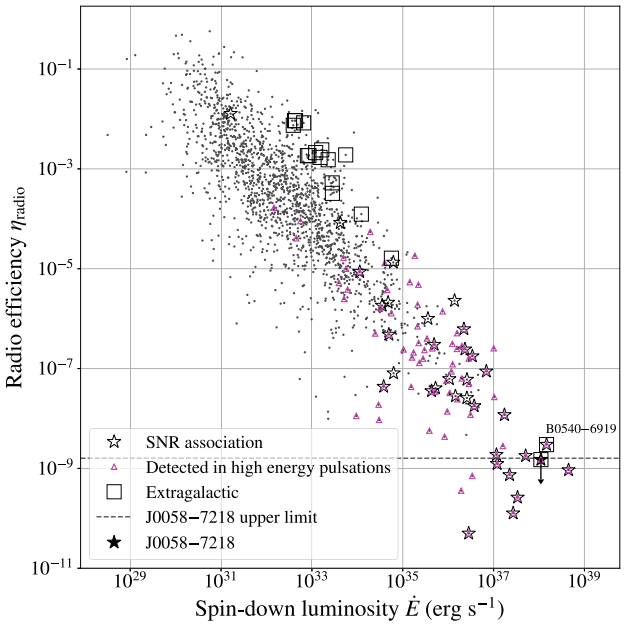

Figure 2. The $\eta_{\rm radio}$–$\dot{E}$ relationship adapted from Szary et al. (2014). PSR J0058−7218 and LMC 'Crab pulsar twin' PSR B0540−6919 are highlighted. As discussed in the text, it is speculative to use a general pulsar luminosity formula to compare individual pulsars' radio efficiencies.

As described in Maitra et al. (2021), the fact that no thermal X-rays are detected from the pulsar, only non-thermal, could mean that the polar cap region (where thermal X-rays are emitted due to accelerated ions colliding with the surface) is not visible. Hence the beam of the radio emission could be missed (Goldreich 1969; Cheng, Gil & Zhang 1998), and no pulses or giant pulses detected. The radio beam could also be intersected at a wide angle where the emission is faint. Indeed, young, short period pulsars can have wide radio beaming angles (e.g. Lyne & Manchester 1988). Since the radio, X-ray, and gamma-ray beams can all have different orientations, the gamma-ray beam could also be missed (e.g.v Cheng & Zhang 1999; Barnard, Venter & Harding 2016). According to Smith et al. (2019), PSR J0058−7218 is near the putative gamma-ray emission 'death line' [with $\dot{E} = 1.1 \times 10^{38}\,\rm erg\,s^{-1}$ (Maitra et al. 2021) and a distance of 60 kpc], and thus could have no gamma-ray emission detectable at all. In the case this 'death line' is an artefact of pulsar distance, the gamma-ray emission could be too faint to be detected with *Fermi*.

PSR J0058−7218 thus joins a growing population of young pulsars with no radio detection. In the current ATNF pulsar catalogue, only half of the ≃50 young pulsars with SNR association are detected in both high-energy and radio pulsations, a quarter are detected only in high-energy pulsations and a quarter only in radio pulsations, with no particular distribution on the period-period derivative plane. There are only two other known extragalactic pulsars in SNRs. Both are in PWNe of the Large Magellanic Cloud. PSR J0537−6910, a fast

[15]The pulsed X-rays are from the pulsar's emission beam, not from any heating processes from the pulsar surface or nebula.
[16]The largest characteristic age of the eight pulsars is 42 kyr.

(16 ms) pulsar, is only[17] detected in X-rays (Marshall et al. 1998), just like PSR J0058−7218. PSR B0540−6919 is detected in X-rays, radio, and gamma-rays and is considered an analogue of the Crab pulsar (Seward, Harnden & Helfand 1984; Manchester et al. 1993; Marshall et al. 2016). It is a giant pulse emitter (Johnston & Romani 2003). It has a very low radio efficiency of $\eta_{\rm radio} = 2.9 \times 10^{-9}$, of the same order as the upper limit on the radio efficiency of PSR J0058−7218. There is only one other extragalactic young[18] non-magnetar pulsar known: J0534−6703 (Manchester et al. 2006). It is a long period ($\simeq$1.8 s) radio pulsar with no SNR or PWN association and no high-energy emission known. There are no confirmed central compact objects (CCO) in the Magellanic Clouds (e.g. Long, Gaetz & Plucinsky 2020). CCOs are soft thermal X-ray sources near the centre of an SNR, with no hard X-ray emission, radio emission, or PWN environment (De Luca 2017).

4 CONCLUSION

We conclude from our unprecedentedly deep radio search that the X-ray pulsar J0058−7218 is either similar to a handful of pulsars in PWNe with very low radio efficiency or its radio beam does not cross our line of sight. The latter hypothesis is supported by the non-detection of thermal X-rays from the polar cap of PSR J0058−7218 in Maitra et al. (2021), and the non-detection of giant pulses in this study. Only about half of young pulsars with SNR associations have been detected in both high-energy and radio pulsations. The upper limit set on PSR J0058−7218's radio flux density in this work is nearly seven times deeper than previous searches. The MeerKAT full array, or the future Square Kilometer Array, could carry out a deeper search on this source. The MeerKAT full array could improve the search sensitivity by a factor of $\simeq$1.5 compared to this work with 20 additional dishes. If PSR J0058−7218 was not detected in a deeper search with the full array, this would not significantly strengthen the case for a non-alignment, as its radio efficiency upper limit would still be higher than seven pulsars. There are only about 20 radio pulsar-PWN systems in the Milky Way. If it was detected, PSR J0058−7218 would be the second extragalactic radio pulsar-PWN system (after PSR B0540−6919 in the Large Magellanic Cloud; Manchester et al. 1993), and the first in the SMC.

ACKNOWLEDGEMENTS

The MeerKAT telescope is operated by the South African Radio Astronomy Observatory, which is a facility of the National Research Foundation, an agency of the Department of Science and Innovation. SARAO acknowledges the ongoing advice and calibration of Global Positioning Systems by the National Metrology Institute of South Africa (NMISA) and the time space reference systems department of the Paris Observatory. TRAPUM observations used the FBFUSE (Filterbank BeamFormer User-Supplied Equipment) and APSUSE (Accelerated Pulsar Searching) computing clusters for data acquisition, storage and analysis. These clusters were funded and installed by the Max-Planck-Institut für Radioastronomie and the Max-PlanckGesellschaft. EC acknowledges funding from the United Kingdom's Research and Innovation Science and Technology Facilities Council (STFC) Doctoral Training Partnership, project reference 2487536. For the purpose of open access, the author has applied a Creative Commons Attribution (CC BY) licence to any Author Accepted Manuscript version arising. EB, MK, PVP, and VVK acknowledge continuing support from the Max Planck Society. RPB acknowledges support from the European Research Council under the European Union's Horizon 2020 research and innovation programme (grant agreement No. 715051; Spiders). We thank Fabian Jankowski and James Turner (Pulsar and Time-Domain Astrophysics group, Jodrell Bank Centre for Astrophysics, University of Manchester) for their help with the primary beam model and the sky temperature estimation, respectively. This paper has made use of the ATNF pulsar catalogue version 1.67. We thank the anonymous referee for their helpful and constructive comments which improved this manuscript.

DATA AVAILABILITY

The data underlying this article will be shared upon reasonable request to the TRAPUM collaboration.

REFERENCES

Abramowski A. et al., 2012, A&A, 545, L2
Asad K. M. et al., 2021, MNRAS, 502, 2970
Bailes M. et al., 2020, Publ. Astron. Soc. Aust., 37, e028
Barnard M., Venter C., Harding A. K., 2016, Proceedings of 4th Annual Conference on High Energy Astrophysics in Southern Africa – PoS(HEASA 2016). Cape Town, South Africa, p. 042
Barsdell B. R., Bailes M., Barnes D. G., Fluke C. J., 2012, MNRAS, 422, 379
Becker W., Trümper J., 1997, A&A, 326, 682
Bochenek C. D., Ravi V., Belov K. V., Hallinan G., Kocz J., Kulkarni S. R., McKenna D. L., 2020, Nature, 587, 59
Caleb M., Keane E., 2021, Universe, 7, 453
Chen W., Barr E., Karuppusamy R., Kramer M., Stappers B., 2021, J. Astron. Instrum., 10, 2150013
Cheng K. S., Zhang L., 1999, ApJ, 515, 337
Cheng K. S., Gil J., Zhang L., 1998, ApJ, 493, L35
Clarke J. N., Little A. G., Mills B. Y., 1976, Aust. J. Phys. Astrophys. Suppl., 40, 1
Cordes J. M., Lazio T. J. W., 2002, in Clemens D., Shah R. Y., Brainerd T., eds, ASP Conf. Ser. Vol. 317, Milky Way Surveys: The Structure and Evolution of Our Galaxy. Astron. Soc. Pac., San Francisco
Crawford F., Kaspi V. M., Manchester R. N., Lyne A. G., Camilo F., D'Amico N., 2001, ApJ, 553, 367
Crawford F., Lorimer D. R., Devour B. M., Takacs B. P., Kondratiev V. I., 2009, ApJ, 696, 574
Davies R. D., Elliott K. H., Meaburn J., 1976, Mem. R. Astron. Soc., 81, 89
De Luca A., 2017, J. Phys.: Conf. Ser., 932, 012006
Esposito P., Rea N., Israel G. L., 2021, Timing Neutron Stars: Pulsations, Oscillations and Explosions. Springer, Berlin, Heidelberg, p. 97
Gendreau K. C. et al., 2016, in den Herder J.-W. A., Takahashi T., Bautz M., eds, Proc. SPIE Conf. Ser. Vol. 9905, Space Telescopes and Instrumentation 2016: Ultraviolet to Gamma Ray. SPIE, Bellingham, p. 99051H
Goldreich P., 1969, Publ. Astron. Soc. Aust., 1, 227
Harris J., Zaritsky D., 2004, AJ, 127, 1531
Heger A., Fryer C. L., Woosley S. E., Langer N., Hartmann D. H., 2003, ApJ, 591, 288
Helfand D. J., Long K. S., 1979, Nature, 282, 589
Henize K. G., 1956, ApJS, 2, 315
Ho W. C. G. et al., 2022, ApJ, 939, 7
Hobbs G. B., Edwards R. T., Manchester R. N., 2006, MNRAS, 369, 655
Hotan A. W., Van Straten W., Manchester R. N., 2004, Publ. Astron. Soc. Aust., 21, 302
Inoue H., Koyama K., Tanaka Y., 1983, in Danziger J., Gorenstein P., eds, Symposium - International Astronomical Union , Volume 101: Supernova

[17]Unpulsed gamma-rays from the PWN have been detected (Abramowski et al. 2012).
[18]All other published non-magnetar extragalactic pulsars are over 200 kyr in characteristic age (Manchester et al. 2005).

Remnants and Their X-Ray Emission, Proc. IAU Symp. Cambridge University Press, Cambridge, p. 535
Jankowski F., van Straten W., Keane E. F., Bailes M., Barr E. D., Johnston S., Kerr M., 2018, MNRAS, 473, 4436
Johnston S., Romani R. W., 2003, ApJ, 590, L95
Joseph T. D. et al., 2019, MNRAS, 490, 1202
Karachentsev I. D., Karachentseva V. E., Huchtmeier W. K., Makarov D. I., 2004, AJ, 127, 2031
Kargaltsev O., Misanovic Z., Pavlov G. G., Wong J. A., Garmire G. P., 2008, ApJ, 684, 542
Keith M. J. et al., 2010, MNRAS, 409, 619
Lamb R. C., Fox D. W., Macomb D. J., Prince T. A., 2002, ApJ, 574, L29
Levin L., 2012, PhD thesis, Swinburne University
Long X., Gaetz T. J., Plucinsky P. P., 2020, ApJ, 904, 70
Lorimer D. R., Kramer M., 2005, Handbook of Pulsar Astronomy. Cambridge University Press, Cambridge
Lyne A. G., Manchester R. N., 1988, MNRAS, 234, 477
McConnell D., McCulloch P. M., Hamilton P. A., Abies J. G., Hall P. J., Jacka C. E., Hunt A. J., 1991, MNRAS, 249, 654
McMahon P. L., 2011, Master's thesis, University of Cape Town,
Maggi P. et al., 2019, A&A, 631, A127
Maitra C., Ballet J., Filipovic M. D., Haberl F., Tiengo A., Grieve K., Roper Q., 2015, A&A, 584, A41
Maitra C., Esposito P., Tiengo A., Ballet J., Haberl F., Dai S., Filipović M. D., Pilia M., 2021, MNRAS, 507, L1
Manchester R. N., Mar D. P., Lyne A. G., Kaspi V. M., Johnston S., 1993, ApJ, 403, L29
Manchester R. N., Hobbs G. B., Teoh A., Hobbs M., 2005, AJ, 129, 1993
Manchester R. N., Fan G., Lyne A. G., Kaspi V. M., Crawford F., 2006, ApJ, 649, 235
Marshall F. E., Gotthelf E. V., Zhang W., Middleditch J., Wang Q. D., 1998, ApJ, 499, L179
Marshall F. E., Guillemot L., Kust Harding A., Martin P., Smith D. A., 2016, American Astronomical Society, AAS Meeting #227, id.423.04
Mathewson D. S., Ford V. L., Dopita M. A., Tuohy I. R., Mills B. Y., Turtle A. J., 1984, ApJS, 55, 189
Mills B., Aller L., 1971, Aust. J. Phys., 24, 609
Mills B. Y., Little A. G., Durdin J. M., Kesteven M. J., 1982, MNRAS, 200, 1007
Morello V., Barr E. D., Stappers B. W., Keane E. F., Lyne A. G., 2020, MNRAS, 497, 4654
Morello V., Rajwade K. M., Stappers B. W., 2021, MNRAS, 510, 1393
Owen R. A. et al., 2011, A&A, 530, A132
Ransom S., 2011, Astrophysics Source Code Library, record ascl:1107.017
Ransom S. M., Eikenberry S. S., Middleditch J., 2002, AJ, 124, 1788
Seward F. D., Mitchell M., 1981, ApJ, 243, 736
Seward F. D., Harnden F. R. J., Helfand D. J., 1984, ApJ, 287, L19
Shibata S., Watanabe E., Yatsu Y., Enoto T., Bamba A., 2016, ApJ, 833, 59
Smith D. A. et al., 2019, ApJ, 871, 78
Stappers B., Kramer M., 2016, in Taylor R., Camilo F., Leeuw L., Moodley K., eds, Proceedings of MeerKAT Science: On the Pathway to the SKA – PoS(MeerKAT2016). Stellenbosch, South Africa, p. 009
Staveley-Smith L. et al., 1996, Publ. Astron. Soc. Aust., 13, 243
Szary A., Zhang B., Melikidze G. I., Gil J., Xu R. X., 2014, ApJ, 784, 59
Taylor J. H., Huguenin G. R., 1969, Nature, 221, 816
Titus N., Stappers B. W., Morello V., Caleb M., Filipović M. D., McBride V. A., Ho W. C. G., Buckley D. A. H., 2019, MNRAS, 487, 4332
Titus N., Toonen S., McBride V. A., Stappers B. W., Buckley D. A., Levin L., 2020, MNRAS, 494, 500
Van Der Heyden K. J., Bleeker J. A., Kaastra J. S., 2004, A&A, 421, 1031
Van Straten W., Bailes M., 2011, Publ. Astron. Soc. Aust., 28, 1
Voraganti Padmanabh P., 2021, PhD thesis, Rheinische Friedrich-Wilhelms-Universität Bonn
Wang W., Zhao Y., 2004, ApJ, 601, 1038
Yao J. M., Manchester R. N., Wang N., 2017, ApJ, 835, 29
Zheng H. et al., 2017, MNRAS, 464, 3486
Zhu W. W. et al., 2014, ApJ, 781, 117

This paper has been typeset from a TEX/LATEX file prepared by the author.